Check for updates

A Journal of the Gesellschaft Deutscher Chemiker

Angewandte International Edition GDCh Chemie

www.angewandte.org

Accepted Article

Title: Advanced low-flammable electrolytes for stable operation of high-voltage lithium-ion batteries

Authors: Hao Jia, Yaobin Xu, Xianhui Zhang, Sarah D Burton, Peiyuan Gao, Bethany E. Matthews, Mark H Engelhard, Kee Sung Han, Lirong Zhong, Chongmin Wang, and Wu Xu

This manuscript has been accepted after peer review and appears as an Accepted Article online prior to editing, proofing, and formal publication of the final Version of Record (VoR). This work is currently citable by using the Digital Object Identifier (DOI) given below. The VoR will be published online in Early View as soon as possible and may be different to this Accepted Article as a result of editing. Readers should obtain the VoR from the journal website shown below when it is published to ensure accuracy of information. The authors are responsible for the content of this Accepted Article.

To be cited as: *Angew. Chem. Int. Ed.* 10.1002/anie.202102403

Link to VoR: https://doi.org/10.1002/anie.202102403

WILEY-VCH

10.1002/anie.202102403

WILEY-VCH

RESEARCH ARTICLE

Advanced low-flammable electrolytes for stable operation of high-voltage lithium-ion batteries

Hao Jia,[a] Yaobin Xu,[b] Xianhui Zhang,[a] Sarah D. Burton,[b] Peiyuan Gao,[c] Bethany E. Matthews,[a] Mark H. Engelhard,[b] Kee Sung Han,[c] Lirong Zhong,[a] Chongmin Wang,[b] Wu Xu [a]*

[a] Dr. H. Jia, Dr. X.H. Zhang, Dr. B.E. Matthews, Dr. W. Xu
Energy and Environment Directorate
Pacific Northwest National Laboratory
902 Battelle Boulevard, Richland, WA 99354, United States
E-mail: wu.xu@pnnl.gov

[b] Dr. Y.B. Xu, Dr. S.D. Burton, M.H. Engelhard, Dr. C.M. Wang
Environmental and Molecular Sciences Laboratory
Pacific Northwest National Laboratory
902 Battelle Boulevard, Richland, WA 99354, United States

[c] Dr. P.Y. Gao, Dr. K.S. Han
Physical and Computational Sciences Directorate
Pacific Northwest National Laboratory
902 Battelle Boulevard, Richland, WA 99354, United States

Supporting information for this article is given via a link at the end of the document.

Abstract: Despite being an effective flame retardant, trimethyl phosphate (TMP_a) is generally considered as an unqualified solvent for fabricating electrolytes used in graphite (Gr) based lithium-ion batteries as it readily leads to Gr exfoliation and cell failure. In this work, by adopting the unique solvation structure of localized high-concentration electrolyte (LHCE) to TMP_a and tuning the composition of the solvation sheathes *via* electrolyte additives, excellent electrochemical performance can be achieved with TMP_a based electrolytes in $Gr||LiNi_{0.8}Mn_{0.1}Co_{0.1}O_2$ cells. After 500 charge/discharge cycles within the voltage range of 2.5-4.4 V, the batteries containing TMP_a based LHCEs with proper additive can achieve a capacity retention of 85.4%, being significantly higher than cells using a $LiPF_6$-organocarbonates baseline electrolyte (75.2%). Meanwhile, due to the flame retarding effect of TMP_a, TMP_a based LHCEs exhibit significantly reduced flammability compared with the conventional $LiPF_6$-organocarbonates electrolyte.

Introduction

Lithium (Li)-ion batteries (LIBs) based on high-nickel (Ni) content $LiNi_xMn_yCo_{1-x-y}O_2$ (NMC, $x \geq 0.6$) positive electrodes have drawn intensive attentions from both scientific and industrial communities as they offer high energy density when operated at relatively high cut-off voltages (> 4.3 V). However, the increased energy density is usually associated with shortened cycle life and aggravated safety hazards.[1] According to the comparative studies performed by Noh *et al.*, thermal runaway can be more easily triggered under abusive conditions for LIBs with higher energy density.[1a] The consequence could be devasting if a flammable electrolyte is used under the violent release of energy during thermal runaway. As the pivotal component in LIBs, the liquid electrolyte plays a determining role in both safety property and electrochemical performance of the LIBs. In the cell chemistry of high-Ni NMC based LIBs operated at high cut-off voltages, the state-of-the-art $LiPF_6$-organocarbonate based electrolytes are considered as incompatible due to their high flammability, low chemical stabilities and inferior solid electrolyte interphases (SEIs).[2]

The conventional approach to reduce the flammability of the $LiPF_6$-organocarbonates electrolytes is to introduce a certain amount of flame retardant (FR) as an additive or a co-solvent.[3] Due to their miscibility with conventional $LiPF_6$-organocarbonates electrolytes and high flame retarding efficiency, phosphorus (P)-based organic compounds, including phosphates, phosphites, phosphonates, phosphazenes, are the most common FRs used in LIBs.[3] Despite their effectiveness in suppressing the flammability of the liquid electrolytes, these compounds generally show incompatibility with the graphite (Gr) negative electrodes. To balance the cycle life and the safety property of the LIBs, the content of the FR in the liquid electrolyte is usually limited to a relatively low content. For instance, trimethyl phosphate (TMP_a) has long been considered as an effective FR for the electrolytes used in LIBs. However, when the content of TMP_a increases beyond 10 wt.% in a conventional electrolyte of 1.0 M $LiPF_6$ dissolved in ethylene carbonate (EC) and ethyl methyl carbonate (EMC) containing vinylene carbonate (VC) as additive, the detrimental impact of TMP_a on the cycling performance of LIBs cannot be neglected (See Figure S1). The reason behind such a phenomenon can be assigned to the interference of TMP_a to the formation of effective SEI on Gr. It is generally accepted that SEI is mainly comprised of the insoluble decomposition products of the cation solvation sheath. As the content of TMP_a increases in the $LiPF_6$-organocarbonates electrolyte, the solvation sheath changes from Li^+-$(EC/VC)_{3-5}$ to $(TMP_a)_m$-Li^+-$(EC/VC)_n$ (See Figure S2). As the decomposition products of such ion sheath do not constitute an effective SEI, continuous electrolyte decomposition on Gr surface and ion sheath co-intercalation into graphene layers of Gr particles take place. It has been recently reported that the introduction of 1,3,2-Dioxathiolane 2,2-dioxide (DTD) can effectively suppress the Gr exfoliation caused by dilute $LiPF_6$-TMP_a electrolyte in potassium ion batteries.[4] However, the applicability of the $LiPF_6$-TMP_a-DTD electrolyte has not yet been verified in LIBs.

This article is protected by copyright. All rights reserved.

Accepted Manuscript

10.1002/anie.202102403

New classes of electrolytes developed in recent years, including high concentration electrolytes and localized high-concentration electrolytes (LHCEs), exhibit many intriguing properties, such as extended anodic stability and effective SEI formation on Li and Gr electrodes.[5] The solvents that were previously considered incompatible with Gr, such as 1,2-dimethoxyethane (DME), can be enabled as qualified electrolyte solvents by the unique solvation structure of LHCEs. In our previous report,[6] an LHCE based on lithium bis(fluorosulfonyl)imide (LiFSI) as salt, triethyl phosphate (TEP_a) as solvating solvent and bis(2,2,2-trifluoroethyl) ether (BTFE) as diluent was developed for Gr based LIBs. However, the Gr||NMC811 cells using TEP_a based LHCE exhibit a relatively low specific capacity, even after an electrolyte additive (EC) is introduced. In addition, compared with the H atoms in the CH_3 groups in TMP_a, the H atoms in the CH_2 groups in TEP_a are prone to be oxidized, limiting the high voltage application of the electrolyte of LiFSI in TEP_a-BTFE. Furthermore, the high volatility of BTFE poses a challenge to the electrolyte preparation and cell assembly. To overcome these disadvantages, TMP_a and 1,1,2,2-tetrafluoroethyl 2,2,3,3-tetrafluoropropyl ether (TTE) were employed as replacements for TEP_a and BTFE, respectively. With the introduction of a small amount of electrolyte additive, TMP_a based LHCE achieved superior cycle life to the state-of-the-art $LiPF_6$-organocarbonates electrolyte in Gr||NMC811 cells operated at the upper cut-off voltage of 4.4 V. Meanwhile, as TMP_a is used at a relatively high content, the flammability of the electrolytes can be significantly reduced.

Results and Discussion

A typical $LiPF_6$-oraganocarbonate electrolyte, 1.0 M $LiPF_6$ in EC-EMC (3:7 by wt.) + 2 wt.% VC (hereinafter, E-Baseline) was selected as the benchmark electrolyte. Four TMP_a based LHCEs were prepared by mixing a high concentration electrolyte of LiFSI in TMP_a with the diluent TTE and an electrolyte additive: 1) no additive, 2) VC, 3) EC and 4) fluoroethylene carbonate (FEC). The detailed electrolyte formulae are summarized in Table 1.

Table 1. Codes and formulae of studied electrolytes

Code	Composition
E-Baseline	1.00 M $LiPF_6$ in EC-EMC (3.0 : 7.0 by wt.) + 2.0 wt.% VC
E-TMP_a	1.44 M LiFSI in TMP_a-TTE (1.4 : 3.0 by mol.)
E-TMP_a-V	1.44 M LiFSI in TMP_a-VC-TTE (1.2 : 0.2 : 3.0 by mol.)
E-TMP_a-E	1.44 M LiFSI in TMP_a-EC-TTE (1.2 : 0.2 : 3.0 by mol.)
E-TMP_a-F	1.44 M LiFSI in TMP_a-FEC-TTE (1.2 : 0.2 : 3.0 by mol.)

Prior to the electrochemical performance evaluations in batteries, the flammability of the studied electrolytes was measured with ignition test.

As shown in Figure 1, the conventional $LiPF_6$-organocarbonate based electrolyte (E-Baseline) can be readily ignited by the flame, and the combustion is self-sustaining. Besides the flammability evaluation on the E-Baseline, the effectiveness of direct introduction of TMP_a into the E-Baseline was also studied (Figure S3). The addition of 10 wt.% TMP_a into the E-Baseline could not fully suppress the flammability of the electrolyte. In comparison, the TMP_a based LHCEs (E-TMP_a, E-TMP_a-V, E-TMP_a-E, E-TMP_a-F) cannot be ignited by the external heating source. The reason can be assigned to the presence of a large amount of TMP_a in these electrolytes. When heated, phosphorus based free radicals are released by the pyrolysis of TMP_a, which neutralize the hydrogen and oxygen based radicals that are indispensable for combustion.[7] Due to the large amount of TMP_a in the electrolytes, all the TMP_a based LHCEs exhibit significantly lower flammability than the E-Baseline and even the E-Baseline+10 wt.% TMP_a. The videos of the flammability measurements were recorded and are included as the supplementary information (Supplementary Videos 1-5).

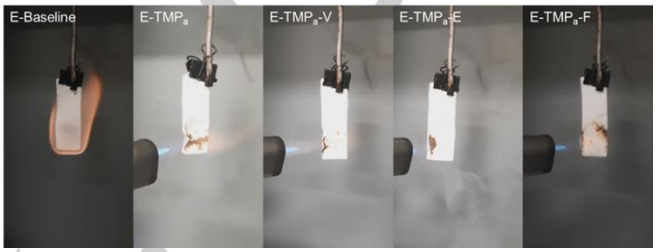

Figure 1. Flammability of the electrolytes listed in Table 1 determined by ignition test.

As stated in introduction, TMP_a is detrimental to the formation of effective SEI on Gr electrodes in conventional $LiPF_6$-organocarbonates electrolytes. After the introduction of 10 wt.% TMP_a into the conventional $LiPF_6$-organocarbonates electrolyte, the electrochemical performance of the Gr||NMC811 cells deteriorates severely (Figure S1).

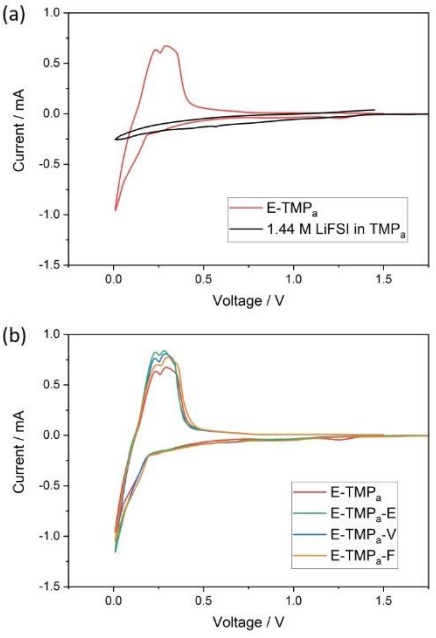

Figure 2. CV curves of Li||Gr cells using (a) 1.44 M LiFSI in TMP_a and 1.44 M LiFSI in TMP_a-TTE (1.4:3.0 by mol.) (E-TMP_a) and (b) all four studied TMP_a based LHCEs.

This article is protected by copyright. All rights reserved.

Accepted Manuscript

10.1002/anie.202102403

To enable TMP_a as a qualified electrolyte solvent used in Gr||NMC811 LIBs of long cycle life, it is indispensable to resolve the incompatibility issue between TMP_a and Gr electrode. Based on previous studies, adjusting the solvation structure of the electrolyte is one of the most effective approaches to enhance the compatibility between the electrolyte solvent and Gr.[8] Herein, the LHCE approach was adopted to TMP_a to resolve its incompatibility issue with Gr. To illustrate the effectiveness of the LHCE, E-TMP_a [*i.e.* 1.44 M LiFSI in TMP_a-TTE (1.4:3.0 by mol.)] and 1.44 M LiFSI in TMP_a were injected into Li||Gr cells and the SEI formation effectiveness was compared with cyclic voltammetry (CV), as shown in Figure 2a.

As demonstrated in Figure 2a, the electrolyte of 1.44 M LiFSI in TMP_a cannot form an effective SEI on Gr, which is consistent with the results reported in previous literature that a dilute salt-TMP_a electrolyte is not compatible with Gr electrodes.[9] However, after substituting part of TMP_a with a non-solvating solvent, TTE (turning the electrolyte into LHCE), an SEI that allows reversible lithiation/delithiation of Gr electrode is formed, despite that the 1.44 M LiFSI in TMP_a electrolyte has the same LiFSI concentration as E-TMP_a. It is well acknowledged that the composition and the structure of the solvation sheath (especially those of the cation sheath) are the two dominant factors over the formation of SEI. The partial substitution of TMP_a by TTE resolved the issue of incompatibility with Gr by changing the solvation structure, which will be discussed in more details in the following section. Besides successfully addressing the incompatibility issue between TMP_a and Gr, E-TMP_a also effectively suppressed the anodic dissolution of Al electrodes, whereas the 1.44 M LiFSI in TMP_a failed (see Figure S4).

The influence of electrolyte additives in E-TMP_a on the compatibility with Gr electrode was also studied. Figure 2b depicts the CV plots of Li||Gr cells comprising the additive containing LHCEs. Apparently, after the introduction of electrolyte additive into E-TMP_a, effective SEIs can be formed in all the additive containing LHCEs.

To understand why the TMP_a is capable of forming an effective SEI in the LHCE, it is necessary to understand the microscopic solvation structures of the TMP_a based LHCEs. *Ab initio* molecular dynamics (AIMD) simulations and diffusion ordered nuclear magnetic resonance spectroscopy (DOSY NMR) were performed to elucidate the solvation structures of these LHCEs.

According to AIMD simulations (Figure 3a), Li^+, FSI^-, and TMP_a are closely packed into ion clusters in E-TMP_a. After the addition of a small amount of electrolyte additive (EC, VC or FEC), the cluster-like structure of the solvation sheath is not damaged, since the electrolyte additive is incorporated into the ion cluster due to their high affinity towards Li^+ (Figure 3b-d). Although the cluster-like solvation structure of the ion sheathes are not changed, the composition of the ion sheathes is tuned by the introduction of different electrolyte additives. Due to the relative scarcity of TMP_a molecules to Li salt, the non-coordinated TMP_a (or so-called "free" TMP_a) cannot be observed in all the TMP_a based LHCEs.

In the LHCEs, the formation of ion clusters resembles the microphase separation in an microemulsion, *i.e.*, each cluster can be treated as a microscopic droplet of high concentration electrolyte. The reason for the formation of such unique solvation structure in LHCEs lies in the highly distinctive polarities between diluent solvent (TTE) and other species, such as LiFSI, TMP_a (and additives). As suggested by the radial distribution function (Figure S5), the coordination bonds between Li^+ and TMP_a, FSI^- or additives are quite strong. In comparison, TTE exhibits very faint affinity (if any) towards Li^+ (Figure S5) due to the low polarity originated from its highly fluorinated structure. The polarity of the diluent (TTE) is low enough to not compete with other solvent or additive species in LiFSI coordination, yet high enough to avoid the phase separation on a macroscopic scale. For this reason, the partial substitution of TMP_a by TTE (from 1.44 M LiFSI in TMP_a to E-TMP_a) has reshaped the microscopic solvation structure and consequently, the electrochemical behavior of the TMP_a based LHCEs.

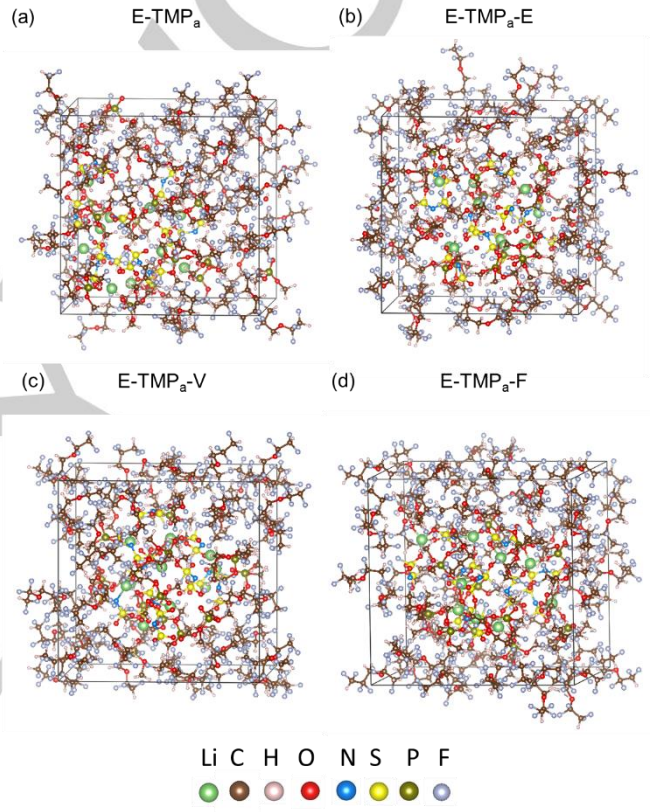

Figure 3. Solvation structures of TMP_a based LHCEs with and without additives obtained from AIMD simulations: (a) no additive, (b) EC, (c) VC, and (d) FEC.

To obtain a deeper understanding of the unique solvation structure of LHCE, DOSY NMR was performed for E-Baseline and E-TMP_a. Based on the spectra, the self-diffusion coefficients of the different species in the electrolytes can be determined.

The self-diffusion coefficients of the major species in E-Baseline were reported in our previous publication.[4b] At 25.0 ℃, the self-diffusion coefficients of Li^+, PF_6^-, EC and EMC in E-Baseline amounted to 1.43×10^{-10}, 2.03×10^{-10}, 2.63×10^{-10} and 3.15×10^{-10} $m^2\ s^{-1}$, respectively (transference number=0.41). In this work, the self-diffusion coefficients of Li^+, TMP_a and FSI^- are determined to be 0.68×10^{-10}, 0.72×10^{-10} and 0.72×10^{-10} $m^2\ s^{-1}$, respectively, being very similar to each other (transference number=0.48). The diffusion coefficient similarity among Li^+, solvating solvent and anion were reported in other LHCE systems as well.[4b, 9] The reason behind such phenomenon can be

This article is protected by copyright. All rights reserved.

Accepted Manuscript

10.1002/anie.202102403

probably assigned to the structural stability of the ion clusters. Due to the strong affinity among the polarized molecules such as Li^+, FSI^-, TMP_a, the ion clusters mainly migrate as a whole in the electrolyte while the molecule exchanges among clusters are not frequent enough to cause significant difference in self diffusion coefficients. Meanwhile, the self-diffusion coefficient of TTE is determined to be 2.75×10^{-10} m^2 s^{-1}, which signifies that the TTE molecules have very weak interaction with the ion-clusters and mainly act as diluent in the system. The self-diffusion coefficients of Li^+, anion, solvating solvent, and diluent in E-TMP_a are lower than their counterparts in E-Baseline, which can be assigned to the relatively high viscosity of the E-TMP_a (Figure S6a). Based on the self-diffusion coefficients and the measured ionic conductivities of the LHCEs (Figure S6b), the dissociation degrees of Li salts can be obtained by the Nernst-Einstein equation.[10]

As depicted in Figure S6b, at the temperature of 25.0 ℃, the ionic conductivities of E-Baseline and E-TMP_a are determined to be 8.9 and 0.81 mS cm^{-1}, respectively. By inputting the ionic conductivities and the self-diffusion coefficients of the Li^+ and anion into the Nernst-Einstein equation, the dissociation degree of $LiPF_6$ in E-Baseline was determined to be 68.8% whereas the dissociation degree of LiFSI in E-TMP_a was determined to be 10.6%. Due to the low dissociation degree, LiFSI molecules predominantly exist as non-dissociated Li^+-FSI^- ion pairs in the ion clusters. During the formation cycles, the Gr electrode is negatively charged, which electrostatically repels the dissociated anions. As $LiPF_6$ in E-Baseline is well dissociated, the anions are not an influential factor in the SEI formation process for E-Baseline. In comparison, most LiFSI exists as non-dissociated ion pairs in the LHCEs, the electrostatic repelling force of negatively charged Gr to anions is buffered by the positively charged Li^+ in the Li^+-$Anion^-$-Solvent clusters. Therefore, anions play a much more active role in SEI formation when LHCEs are used.[5c, 11] Because of the synergetic decompositions of FSI^- and TMP_a in the ion clusters, an effective SEI can be generated on the Gr particles, thus solving the incompatibility issues between TMP_a and the Gr electrodes (see Figure 2).

After confirming the compatibility between TMP_a based LHCEs with Gr electrode, the long-term cycling performance of Gr||NMC811 coin cells using the selected electrolytes was evaluated. As shown in Figure 4, the average specific discharge capacity of the Gr||NMC811 cells comprising E-Baseline amounts to 176.9 mAh g^{-1} after formation cycles. The average capacity of these cells decays monotonously over increasing cycle number. After 500 charge/discharge cycles, the average specific discharge capacity of the cells declines to 133.0 mAh g^{-1}, corresponding to a capacity retention of 75.2%. In contrast, cells using E-TMP_a exhibit a relatively slow capacity decay in the first 190 charge/discharge cycles. Thereafter, the E-TMP_a based cells exhibit a suddenly accelerated capacity fading. After 500 charge/discharge cycles, the average specific capacity of the cell merely amounts to 63.5 mAh g^{-1}, corresponding to the capacity retention of 38.1%. After the introduction of EC (E-TMP_a-E), the initial specific capacity (after formation cycles) of the Gr||NMC811 cells is boosted to 178.6 mAh g^{-1}, being the highest among the studied electrolytes. Such an improvement can be possibly ascribed to the formation of a highly ionically conductive SEI. However, cells using E-TMP_a-E also exhibit the suddenly accelerated capacity decay that sets off even earlier than the additive-free E-TMP_a. The reason behind such a phenomenon can be mainly assigned to the ineffectiveness of the SEI formed in these electrolytes over the long-term, which will be discussed in more details in the later section. In comparison, the introduction of VC and FEC effectively extends the cycle life of the cells. For E-TMP_a-V and E-TMP_a-F based cells, the specific capacities after formation cycles are determined as 137.2 mAh g^{-1} and 164.1 mAh g^{-1}, respectively, which gradually decays to 120.8 mAh g^{-1} and 140.2 mAh g^{-1} after 500 charge/discharge cycles. The capacity retentions of E-TMP_a-V based cells and E-TMP_a-F based cells are determined to be 88.0% and 85.4%, respectively, being much higher than that of E-Baseline cells. It should be noted that the cells using the E-TMP_a-V exhibit a relatively low initial capacity and a capacity increase in the first 50 charge/discharge cycles followed by capacity decay. It indicates that the activation of the Gr||NMC811 cells takes a relatively long time when E-TMP_a-V is used. The high capacity retention of Gr||NMC811 cells comprising E-TMP_a-V partially originates from the long activation step. In comparison, cells using E-TMP_a-F exhibit the best long-term cycling performance among all the studied cells. The Coulombic efficiencies of the studied cells were also compared and discussed in the supporting information (Figure S7).

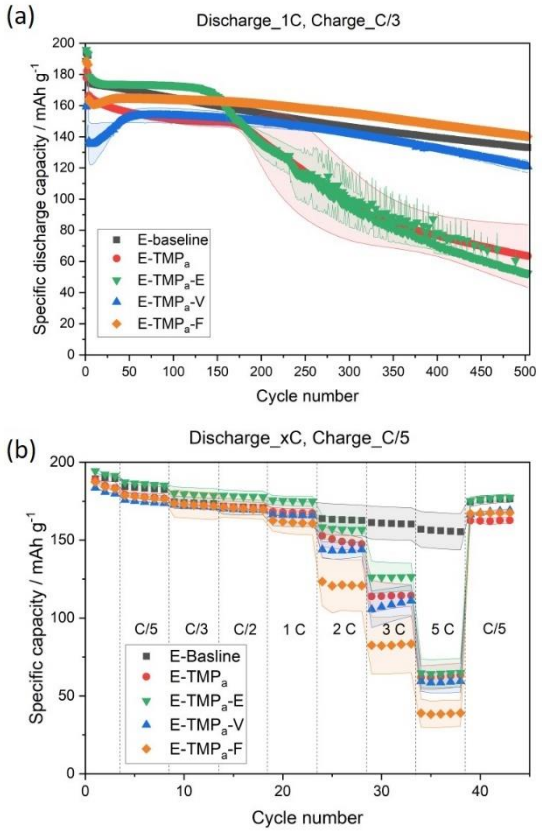

Figure 4. (a) Average specific discharge capacities of Gr||NMC811 cells with studied electrolytes plotted as the function of cycle number; (b) Average specific discharge capacities of Gr||NMC811 cells charged at the constant C-rate of C/5 and discharged at the C-rates of C/5, C/3, C/2, 1C, 2C, 3C, 5C, and C/5, where 1C = 1.66 mA cm^{-2}.

The discharge rate capabilities of Gr||NMC811 cells using the studied electrolytes were evaluated in parallel. As shown in Figure 4b, E-Baseline exhibits the superior discharge rate

This article is protected by copyright. All rights reserved.

Accepted Manuscript

performance to the E-TMP$_a$, E-TMP$_a$-V and E-TMP$_a$-F, especially under the high C-rates of 2C, 3C and 5C. E-TMP$_a$-E achieves a slightly higher capacity than E-Baseline when the C-rate is lower than 2C. The difference between E-Baseline and TMP$_a$ based LHCEs can be assigned to the lower ionic conductivity of the TMP$_a$ based LHCEs and the higher interphasial resistance (see detailed discussions in Figure S8). The relatively low ionic conductivities of LHCEs is an intrinsic issue associated with LHCEs.[4b, 11] Nevertheless, TMP$_a$ based LHCEs can achieve satisfactory electrochemical performance up to 1C, making them favorable for building high energy density LIBs with improved safety features.

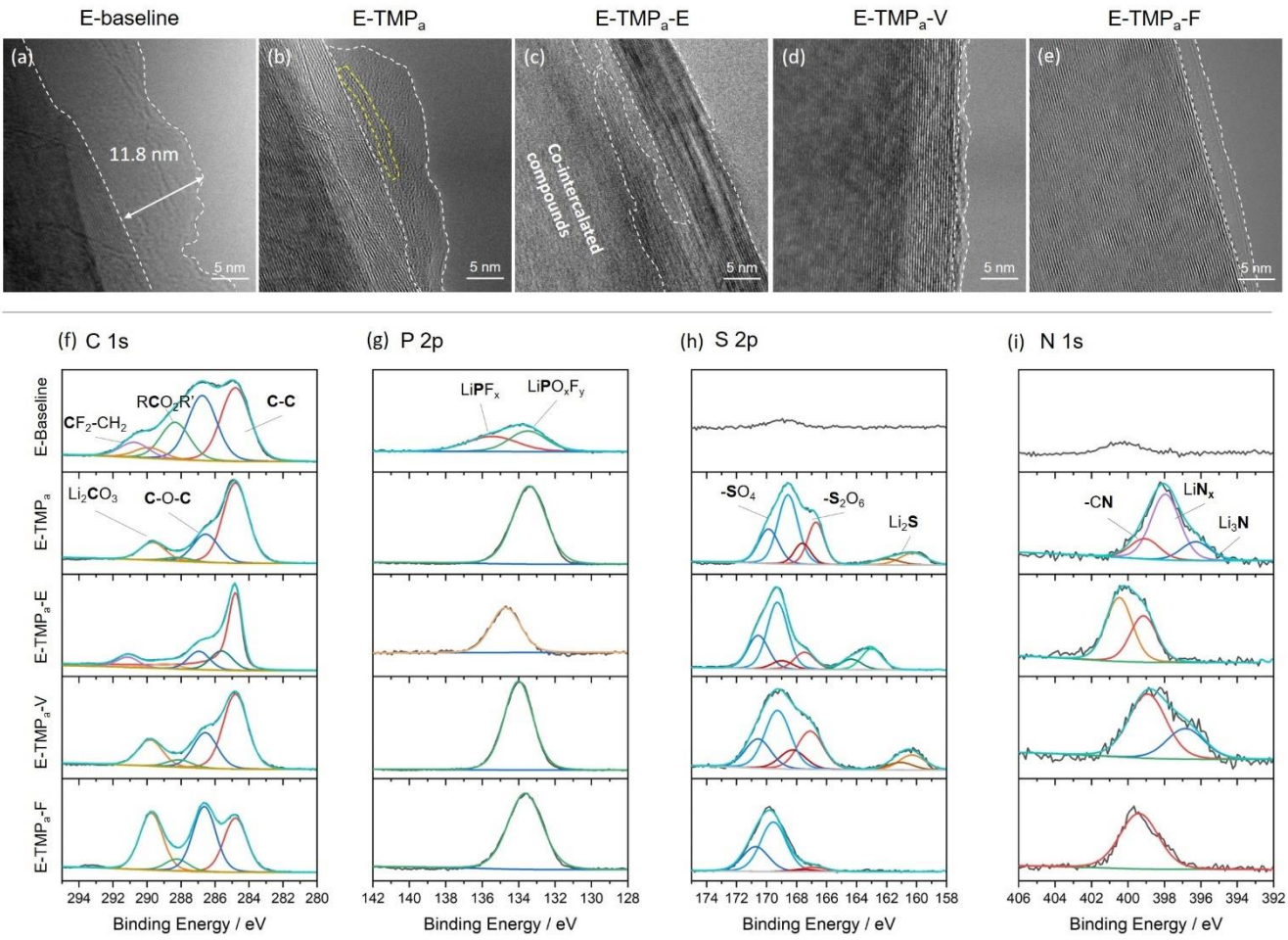

Figure 5. (a-e) Micrographs of Gr particles retrieved from Gr electrodes after being charged/discharged for 500 cycles in the studied electrolytes: (a) E-Baseline, (b) E-TMP$_a$, (c) E-TMP$_a$-E, (d) E-TMP$_a$-V, (e) E-TMP$_a$-F. (f-i) XPS spectra of selected elements of the SEIs on Gr electrodes after being charged/discharged for 500 cycles in the studied electrolytes: (f) C 1s, (g) P 2p, (h) S 2p, (i) N 1s.

With this, it can be concluded the selection of proper electrolyte additive is crucial to achieving long lifespan of Gr||NMC811 cells. Based on the systematic studies, FEC is confirmed to be the most compatible electrolyte additive with the LiFSI-TMP$_a$-based LHCE since E-TMP$_a$-F enables Gr||NMC811 cells to achieve higher specific capacity and higher capacity retention than the E-Baseline over the long-term.

To understand the different aging behaviors of the Gr||NMC811 cells using the selected electrolytes, ex-situ analyses, including X-ray photoelectron spectroscopy (XPS) and transmission electron microscopy (TEM), were performed for the Gr and NMC811 electrodes retrieved from the cycled cells.

The morphologies of the SEIs on cycled Gr electrodes were characterized by TEM. As shown in Figure 5a, the SEI formed in E-Baseline exhibits a non-uniform morphology and the thickness of the SEI is > 10 nm on average. The thick and non-uniform SEI is considered to be the major reason behind the relatively fast capacity decay of the Gr||NMC811 cells using E-Baseline.[4b]

Similarly, a thick and non-uniform SEI can be observed on the surface of Gr particle cycled in E-TMP$_a$ after long-term cycling (see Figure 5b). Moreover, a certain degree of Gr exfoliation can be observed in Figure 5b (marked by yellow broken lines), indicating that the SEI formed in E-TMP$_a$ is not sufficiently protective against co-intercalation over long-term cycling. The introduction of EC into the E-TMP$_a$ electrolyte (i.e. the use of a small amount of EC to replace TMP$_a$ in E-TMP$_a$) does not resolve such an issue (Figure 5c). On the contrary, the Gr exfoliation even aggravates with the EC presence in the electrolyte (E-TMP$_a$-E). As illustrated in Figure 6c, several tens of graphene layers are “afloat” over a large amorphous domain that is originated from

This article is protected by copyright. All rights reserved.

Accepted Manuscript

electrolyte co-intercalation. The disintegration of Gr is considered to be the reason behind the sudden capacity decay of the cells using E-TMP$_a$ and E-TMP$_a$-E (See Figure 4a).

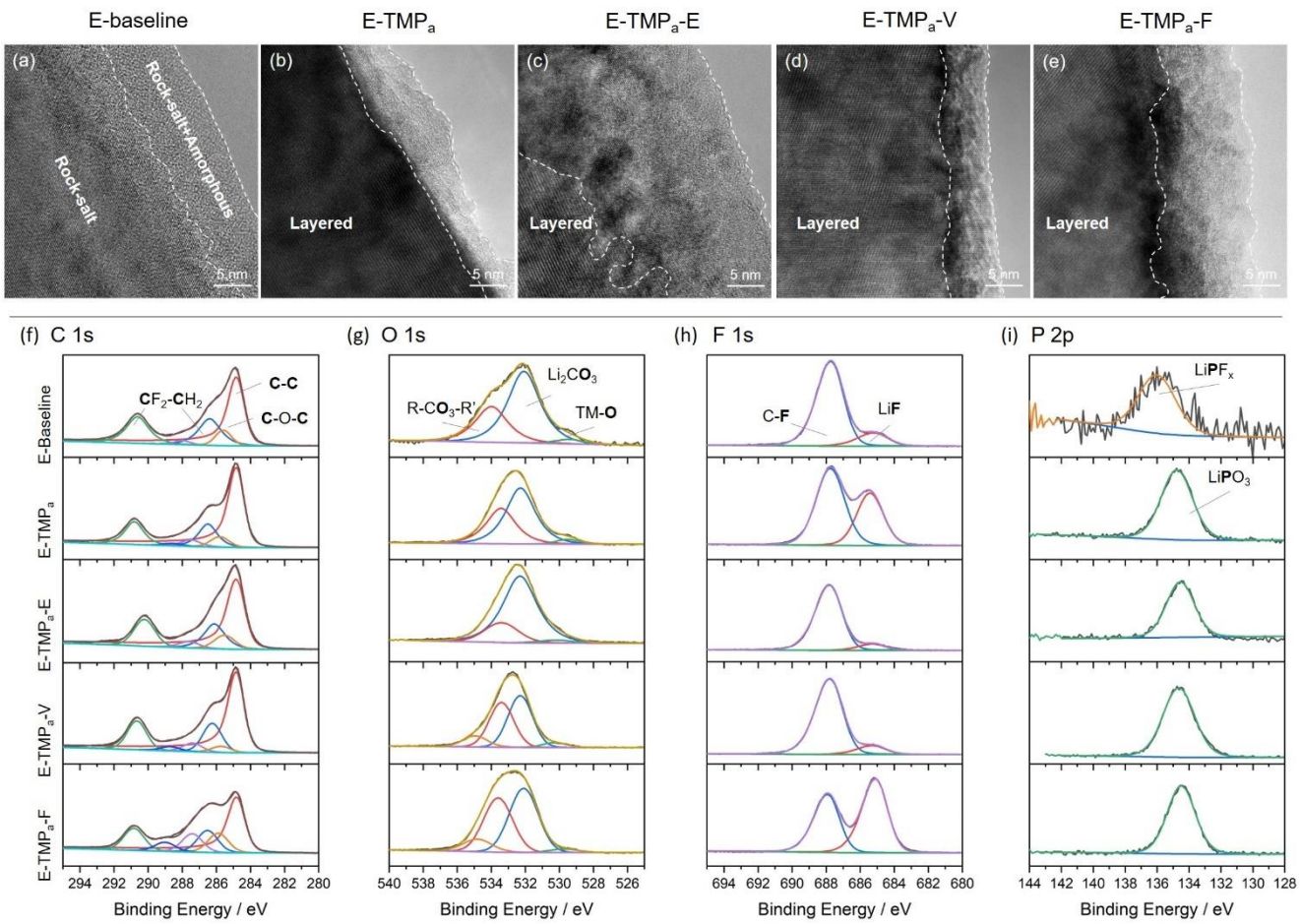

Figure 6. (a-e) TEM images of NMC811 particles after 500 cycles in Gr||NMC811 cells using studied electrolytes: (a) E-Baseline, (b) E-TMP$_a$, (c) E-TMP$_a$-E, (d) E-TMP$_a$-V, (e) E-TMP$_a$-F. (f-i) XPS spectra of selected elements of the CEIs on NMC811 electrodes after being charged/discharged for 500 cycles in the studied electrolytes: (f) C 1s, (g) O 1s, (h) F 1s, (i) P 2p.

In comparison, after using the same small amount of VC or FEC to replace all EC in E-TMP$_a$-E, the Gr exfoliation is effectively suppressed (see Figures 5d and 5e). In E-TMP$_a$-V, the SEI is not uniform in thickness, however, it is quite thin (~ 2 nm), even after 500 charge/discharge cycles. In the case of Gr cycled in E-TMP$_a$-F, a highly uniform and compact SEI layer can be observed. The SEI exhibits a layered structure as a clear boundary is observed within the SEI. Some microscopic crystalline domains are embedded in the SEI. The morphology evolution of the SEIs is well corresponded to the long-term cycling performance of the Gr||NMC811 cells, that cells using E-TMP$_a$ and E-TMP$_a$-E exhibit suddenly accelerated capacity decay whereas those using E-TMP$_a$-V and E-TMP$_a$-F achieve high capacity retentions. These findings reemphasize the significance of effective SEI on the electrochemical performance of Gr based LIBs.

Figures 5f-5i illustrate the XPS spectra of selected elements of the SEIs formed in the studied electrolytes after 500 charge/discharge cycles. All the XPS spectra were calibrated by shifting the C-C peak in the C 1s spectra to the binding energy of 284.8 eV. It should be noted that the spectra of the E-TMP$_a$-E is significantly different from other samples. The reason is that the Gr electrodes were severely exfoliated in E-TMP$_a$-E after long-term cycling. The solvent co-intercalation leads to the morphological and compositional changes of the SEI, which consequently leads to the abnormities in XPS spectra. For this reason, the spectra of the SEI sample formed in E-TMPa-E are not comparable to other samples, so they will not be discussed in detail.

As shown in Figure 5f, the SEI formed in E-Baseline is comprised of a significant portion of ether-like species (C-O-C, 286.6 eV in C 1s spectrum), which corresponds to the common polyethylene oxide (PEO) like species in the SEI.[12] In addition, a significant amount of ester species (288.4 eV in C 1s spectrum) is identified in the SEI formed in E-Baseline, whereas the contents of this species in TMP$_a$ based LHCEs are significantly lower. Compared with the SEI in E-TMP$_a$, the contents of the ester are

This article is protected by copyright. All rights reserved.

Accepted Manuscript

slightly higher in SEIs formed in VC and FEC containing LHCEs: E-TMP_a-V and E-TMP_a-F. It is reasonable to consider that this species originates from the decomposition of the organic carbonates. The higher ester contents in E-TMP_a-V and E-TMP_a-F imply that the additive plays a role in the SEI formation process in the TMP_a-based LHCEs. Li_2CO_3 species was identified in all the samples.

In the P 2p spectra (Figure 5g), significant amounts of P-containing compounds are detected in the SEIs formed in TMP_a based LHCEs. Since P is characteristic to TMP_a in the TMP_a based LHCEs, the presence of P in SEIs confirms that TMP_a participated in the SEI formation. As confirmed previously, the decomposition of TMP_a in the electrolyte of 1.44 M LiFSI in TMP_a interferes with the formation of an effective SEI on Gr. However, after adopting the LHCE concept, reversible lithiation/delithiation of the Gr can be achieved, even when TMP_a was used as the main solvating solvent. The reason for the formation of an effective SEI can be attributed to the participation of FSI^- anions in the SEI formation. As shown in XPS spectra of S 2p (Figure 5h) and N 1s (Figure 5i), the characteristic elements of FSI^-, S and N, are detected in all the SEIs formed in TMP_a based LHCEs. Due to the low dissociation degree of LiFSI in the TMP_a based LHCEs, the anions were promoted to participate in the SEI formation. The synergetic decomposition of TMP_a, FSI^-, and additive effectively addresses the incompatibility issue of TMP_a with Gr electrode. The O 1s and F 1s XPS spectra of the SEIs were also measured. The results and corresponding discussions are summarized in Figure S9.

Based on the XPS spectra, it can be concluded that the SEI in the E-Baseline mainly originates from the decomposition of the Li^+-$(EC/VC)_n$ solvation sheath. In comparison, the anion, the additive and the solvating solvent in TMP_a based LHCEs all play a part in the SEI formation process. The SEIs formed in E-TMP_a-V and E-TMP_a-F are highly effective as they offer good protection against solvent co-intercalation and their thicknesses are much lower than that formed in E-Baseline after long-term cycling performance evaluation. The SEIs formed by the synergy of LiFSI, TMP_a and additive can overcome the disadvantage of TMP_a and ensure the excellent long-term cycling performance of Gr||NMC811 cells.

Besides the SEI, the aging behavior of the cathode electrolyte interphase (CEI) on the positive electrode should also be taken into consideration. The morphologies of CEIs were determined by high resolution TEM after long-term cycling performance evaluation. As shown in Figure 6a, a significant proportion of the NM811 particle has transformed from a layered structure to a mixture of rock-salt phase and amorphous phase after being charged/discharged for 500 cycles in the E-Baseline. The thickness of such a mixture layer is determined to be more than 20 nm. It should be noted that the phase transition of NMC811 particles is an inevitable process, which can be catalyzed by the presence of acidic species.[13] Since $LiPF_6$ inevitably leads to the generation of HF during the operation of the cells, the $LiPF_6$-organocarbonate based electrolyte (E-Baseline) is considered to contribute to the phase change of the NMC811 material.[14] However, because LiFSI is chemically more stable than $LiPF_6$, less acidic species are released into the electrolyte over the long-term cycling. Consequently, the phase transition from layered structure to rock-salt structure is not severe in the cells using TMP_a based LHCEs (Figures 6b to 6e).

In addition to the Li salt, additives may also play a partial role in catalyzing the phase change of the positive electrode materials. For instance, FEC is also capable of generating HF upon cycling. Therefore, the phase transition of NMC811 in E-TMP_a-F is more severe than that in E-TMP_a and E-TMP_a-V. The detrimental effect of FEC on NMC811 was also observed in our previous publication.[5c] Theoretically, the phase change of NMC811 in E-TMP_a-E should also be relatively mild. However, as revealed in Figure 6c, the phase transition of NMC811 in E-TMP_a-E is the worst among all the studied LHCEs. The severe disintegration of Gr in E-TMP_a-E (Figure 5c) probably leads to the generation of various decomposition products of the electrolyte, and these decomposition products consequently lead to a severe phase change of NMC811 in E-TMP_a-E via the detrimental cross-talks from the Gr side to the NMC811.

The compositions of the CEIs formed on the NMC811 materials were characterized by XPS. Compared with the pristine NMC811 material (Figure S10b), the C 1s spectra (Figure 6f) of the NMC811 electrodes only exhibit minor changes, even after being cycled for 500 charge/discharge cycles. The characteristic peaks of the polyvinylidene fluoride (PVDF) binder and conductive carbon can still be observed. It indicates that the contents of the decomposition products of the electrolytes are relatively scarce as the peaks of the original species in the NMC811 electrode are not obscured by the decomposition products of the electrolytes. The reason behind such a phenomenon can be assigned to the anodic stability of the studied electrolytes. As shown in Figure S11, the anodic stabilities of E-Baseline, E-TMP_a, E-TMP_a-E, E-TMP_a-V and E-TMP_a-F were determined to be 4.7 V, 4.9 V, 4.9 V, 4.6 V and 4.9 V (*vs.* Li/Li^+), respectively, being higher than the cut-off voltage of 4.4 V (~4.5 V *vs.* Li/Li^+). In comparison, the formation of SEI obscured most of the original peaks in the pristine Gr (Figure 5f). According to the spectra of O 1s (Figure 6g), F 1s (Figure 6h) and P 2p (Figure 6i), the decomposition products in the E-Baseline were determined to be R-CO_3-R', LiF and $LiPO_xF_y$. In LHCEs, the CEIs are mainly comprised of R-CO_3-R', LiF, $LiPO_3$ and some decomposition products of the FSI^- anions (See Figure S12).

Combing the TEM and XPS results, it can be concluded that the CEI of the NMC811 mainly originates from the phase transition of NMC811. Only a small amount of the electrolyte was decomposed due to the relatively good electrochemical stability of the studied electrolytes.

Conclusion

TMP_a, previously considered to be incompatible with Gr based LIBs, has been successfully enabled as a quantified electrolyte solvent by adopting the concept of LHCE. The relatively high TMP_a content in the electrolyte effectively suppressed the flammability of the electrolyte. Meanwhile, due to the unique solvation structure of the electrolyte, an effective SEI can be formed on Gr electrode by the synergetic decomposition between LiFSI and TMP_a. However, cells using E-TMP_a exhibit sudden capacity decay after approximately 190 charge/discharge cycles. Ex-situ analyses reveal the partial Gr exfoliation is the reason behind such a phenomenon. In response to this challenge, functional electrolyte additives, including EC, VC and FEC, were introduced into E-TMP_a. FEC was proven to be highly effective to resolve the issue. Compared with the conventional $LiPF_6$-

This article is protected by copyright. All rights reserved.

Accepted Manuscript

organocarbonate based electrolyte, the E-TMP_a-F achieved both improved safety property and extended cycle life in Gr||NMC811 cells operated at the cut-off voltage of 4.4 V. For this reason, the electrolyte is of high interest for the fabrication of safe, high energy density LIBs.

Acknowledgements

This work was supported by the U.S. Department of Energy (DOE)'s Office of Energy Efficiency and Renewable Energy (EERE) through the Applied Battery Research Program under the Award Numbers DE-EE0008444 and DE-AC05-76RL01830. The TEM characterizations were supported by Office of Vehicle Technologies of the U. S. DOE under the Advanced Cathode Materials Program (Award Number DE-LC-000L053). The microscopic and spectroscopic characterizations were conducted in the William R. Wiley Environmental Molecular Sciences Laboratory (EMSL), a national scientific user facility sponsored by DOE's Office of Biological and Environmental Research and located at Pacific Northwest National Laboratory (PNNL). PNNL is operated by Battelle for the DOE under Contract DE-AC05-76RL01830. The authors would like to thank Dr. Bryant Polzin of Argonne National Laboratory for supplying the Gr and NMC811 electrodes and Dr. Kazuhiko Murata of Nippon Shokubai Co., Ltd. for providing the LiFSI salt.

Keywords: lithium-ion battery; trimethyl phosphate electrolyte; low flammability; graphite compatibility; long cycle life

[1] (a) H.-J. Noh, S. Youn, C. S. Yoon, Y.-K. Sun, *Journal of power sources* **2013**, *233*, 121-130; (b) G. Xu, L. Huang, C. Lu, X. Zhou, G. Cui, *Energy Storage Materials* **2020,** *31*, 72-86.

[2] K. Beltrop, S. Klein, R. Nölle, A. Wilken, J. J. Lee, T. K.-J. Köster, J. Reiter, L. Tao, C. Liang, M. Winter, *Chemistry of Materials* **2018**, *30*, 2726-2741.

[3] (a) X. Yao, S. Xie, C. Chen, Q. Wang, J. Sun, Y. Li, S. Lu, *Journal of power sources* **2005**, *144*, 170-175; (b) H. Xiang, H. Xu, Z. Wang, C. Chen, *Journal of Power Sources* **2007**, *173*, 562-564; (c) T. Dagger, C. Lürenbaum, F. M. Schappacher, M. Winter, *Journal of Power Sources* **2017**, *342*, 266-272; (d) S. Zhang, K. Xu, T. Jow, *Journal of Power Sources* **2003**, *113*, 166-172; (e) B. Wu, F. Pei, Y. Wu, R. Mao, X. Ai, H. Yang, Y. Cao, *Journal of Power Sources* **2013**, *227*, 106-110.

[4] G. Liu, Z. Cao, L. Zhou, J. Zhang, Q. Sun, J. Y. Hwang, L. Cavallo, L. Wang, Y. K. Sun, J. Ming, *Advanced Functional Materials* **2020**, *30*, 2001934.

[5] (a) Z. Zeng, V. Murugesan, K. S. Han, X. Jiang, Y. Cao, L. Xiao, X. Ai, H. Yang, J.-G. Zhang, M. L. Sushko, *Nature Energy* **2018**, *3*, 674-681; (b) X. Ren, L. Zou, X. Cao, M. H. Engelhard, W. Liu, S. D. Burton, H. Lee, C. Niu, B. E. Matthews, Z. Zhu, C. Wang, B.W. Arey, J. Xiao, J. Liu, J.-G. Zhang, W. Xu, *Joule* **2019**, *3*, 1662-1676; (c) H. Jia, Y. Xu, S. D. Burton, P. Gao, X. Zhang, B. E. Matthews, M. H. Engelhard, L. Zhong, M. E. Bowden, B. Xiao, K. S. Han, C. Wang, W. Xu, *ACS Applied Materials & Interfaces* **2020**, *12*, 54893-54903.

[6] X. Cao, Y. Xu, L. Zhang, M. H. Engelhard, L. Zhong, X. Ren, H. Jia, B. Liu, C. Niu, B. E. Matthews, H. Wu, B.W. Arey, C. Wang, J.-G. Zhang, W. Xu, *ACS Energy Letters* **2019**, *4*, 2529-2534.

[7] B. Schartel, *Materials* **2010**, *3*, 4710-4745.

[8] M. Nie, D. P. Abraham, D. M. Seo, Y. Chen, A. Bose, B. L. Lucht, *The Journal of Physical Chemistry C* **2013**, *117*, 25381-25389.

[9] (a) J. Wang, Y. Yamada, K. Sodeyama, E. Watanabe, K. Takada, Y. Tateyama, A. Yamada, *Nature Energy* **2018**, *3*, 22-29; (b) K. Takada, Y. Yamada, A. Yamada, *ACS applied materials & interfaces* **2019**, *11*, 35770-35776.

[10] K. Hayamizu, *Journal of Chemical & Engineering Data* **2012**, *57*, 2012-2017.

[11] X. Zhang, L. Zou, Y. Xu, X. Cao, M. H. Engelhard, B. E. Matthews, L. Zhong, H. Wu, H. Jia, X. Ren, P. Gao, Z. Chen, Y. Qin, C. Kompella, B. W. Arey, J. Li, D. Wang, C. Wang, J.-G. Zhang, W. Xu, *Advanced Energy Materials* **2020**, *10*, 2000368.

[12] Y. Qian, C. Schultz, P. Niehoff, T. Schwieters, S. Nowak, F. M. Schappacher, M. Winter, *Journal of Power Sources* **2016**, *332*, 60-71.

[13] W. Xuan, A. Otsuki, A. Chagnes, *RSC Advances* **2019**, *9*, 38612-38618.

[14] S. Wiemers-Meyer, S. Jeremias, M. Winter, S. Nowak, *Electrochimica Acta* **2016**, *222*, 1267-1271.

This article is protected by copyright. All rights reserved.

Accepted Manuscript

10.1002/anie.202102403

WILEY-VCH

RESEARCH ARTICLE

Table of contents graphic

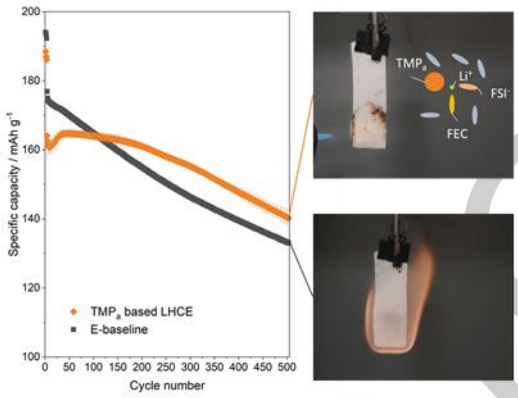

Advanced low-flammable electrolytes are developed for high-voltage lithium-ion batteries (LIBs). With fluoroethylene carbonate as a proper electrolyte additive, the trimethyl phosphate based localized high-concentration electrolyte achieves greatly extended cycle life over the conventional $LiPF_6$-organocarbonates electrolyte, due to the formation of enhanced surface protection layers, making it a promising candidate for high-energy-density LIBs.

WILEY-VCH

Accepted Manuscript

This article is protected by copyright. All rights reserved.